HYDROLOGICAL PROCESSES
Hydrol. Process. (2015)
Published online in Wiley Online Library
(wileyonlinelibrary.com) DOI: 10.1002/hyp.10491

Preferential percolation quantified by large water content sensors with artifactual macroporous envelopes

Ilse Kogelbauer,[1] Kamila Bát'ková,[2] František Doležal,[2]* Svatopluk Matula[2] and Willibald Loiskandl[1]

[1] *Institute of Hydraulics and Rural Water Management, Department of Water, Atmosphere and Environment, University of Natural Resources and Life Sciences (BOKU), Gregor-Mendel-Straße 33, Vienna, 1180, Austria*
[2] *Department of Water Resources, Faculty of Agrobiology, Food and Natural Resources, Czech University of Life Sciences, Kamýcká 129, Praha 6 – Suchdol, 165 21, Czech Republic*

Abstract:

For many scientific and practical tasks, it is important to estimate the soil–water percolation fluxes. This paper builds on measurements with large horizontal time-domain reflectometry water content sensors in a loamy Mollisol. The sensors were installed into pre-drilled holes and the gaps between them, and the soil was filled with a slurry of local soil with water. This gave rise to envelopes around them that contained artificial macropores. The sensors reacted to intensive rains by a rapid increase of their readings, often above the native soil's porosity, followed by an almost equally rapid decrease.

The paper explores the feasibility of quantifying the rapid percolation, based on these anomalous water content peaks, and demonstrates that this is possible in principle, if the processes are simulated by a suitable model. A two-dimensional dual porosity non-equilibrium (mobile-immobile) model was tried. The envelope around the sensor was modelled as an annulus with higher porosity and hydraulic conductivity, which attracts preferential flow and amplifies the percolation signal. With the model at hand, the flux hydrographs can be derived from model simulations and measured precipitation.

For contrast, the Durner equilibrium dual porosity model was tried but was found little suitable. However, even the mobile-immobile model did not perform perfectly. Simulated water contents were similar to the measured ones at some depths but not in the others, and the percolation fluxes were overestimated, compared to cumulative soil–water balance. Efforts to improve model performance were not successful. Hence, the model structure needs to be improved. Copyright © 2015 John Wiley & Sons, Ltd.

KEY WORDS TDR; mobile/immobile water; HYDRUS; permeable annulus; Durner model; water balance

Received 30 October 2013; Accepted 16 March 2015

INTRODUCTION

Whenever one is concerned with the soil–water regime and its practical consequences, e.g. in terms of the soil forming processes or groundwater recharge and pollution, one has to quantify, among other things, the portions of surface water (coming from rain, snowmelt, irrigation, flooding etc.) that are capable of penetrating into different depths in the soil and the speed with which this penetration happens. It is therefore important to be able to determine the soil–water fluxes and their variation in space and time and also to distinguish the preferential percolation from the non-preferential one, as the two processes may have different consequences in terms of soil functions (Clothier *et al*., 2008). In many cases, the preferential and non-preferential fluxes co-exist and collectively contribute to groundwater recharge, which occurs even in very dry climates (Crosbie *et al*., 2010). Some investigations (e.g. Ireson *et al*., 2006; Mathias *et al*., 2006; Pirastru and Niedda, 2010) suggest that the preferential flux makes only a minor part of the total flux in deeper layers of the unsaturated fissured chalk rocks. On the other hand, the preferential flux is a considerably more efficient carrier of pollutants than the non-preferential one (Köhne *et al*., 2009).

Many methods of investigation of preferential flux in soils were recently published. For example, one can refer to the overviews by Allaire *et al*. (2009) and Gerke *et al*. (2010) and also to those by Gerke (2006), Jarvis (2007), Köhne *et al*. (2009) and Beven and Germann (2013) that are focused on concepts and models but also mention measurement methods. It is rarely possible to measure the preferential fluxes directly and continuously, especially under field conditions. The impossibility of direct measurement of fluxes was also noticed, e.g. by Ireson *et al*. (2006). A feasible option, briefly mentioned by

*Correspondence to: František Doležal, Department of Water Resources, Faculty of Agrobiology, Food and Natural Resources, Czech University of Life Sciences, Kamýcká 129, Praha 6 – Suchdol, 165 21, Czech Republic.
E-mail: dolezalf@af.czu.cz

Allaire *et al*. (2009), is to use several soil–water sensors in parallel, in order to continuously monitor the variability of water occurrence in the soil. This variability is, among other factors, affected by the preferential flow (as also noticed, e.g. by Rosenbaum *et al*. (2012)). Allaire *et al*. (2009) suggest that it is more advantageous to place the sensors horizontally and place numerous sensors at small spatial intervals from each other. The sensors must allow continuous monitoring at high temporal frequency so that they can detect short-duration preferential flow events. Moysey and Liu (2012) suggested to detect the preferential flow in macropores using electrical resistivity measurements, while Umarova and Samoilov (2011) used temperature measurements for the same purpose.

Doležal *et al*. (2012a,b; 2015) measured soil–water content by large time-domain reflectometry (TDR) sensors that had been installed horizontally in a loamy Udic Haplustoll. They found that the TDR readings become very high for some time during and after intensive rainfall and snowmelt events. These readings were perceivably higher than those before the percolation event and sometimes even higher than the saturated water content of the soil. Typically, the anomalously high TDR reading quickly fell down as soon as the percolation event was over. The cited authors interpreted the phenomenon qualitatively in terms of preferential percolation through the macropores of the native soil and the artificial macropores and gaps between the sensors and the native soil, assuming that a temporary accumulation of water near the sensor was preferentially detected and made them a sort of amplifiers of the percolation signal. Doležal *et al*. (2012a,b; 2015) conclude that the anomalous and short-lasting water content peaks are indicators of the rapid downward percolation, which is very probably of preferential (i.e. non-equilibrium) nature. The same authors envisage that sensors of this type could be used for a safe qualitative detection of the preferential flow and, perhaps, also for its quantification, assuming that the magnitude of the effect described previously can be related to the magnitude of the preferential flux.

Adamsen and Hunsaker (2000) and Zhao *et al*. (2006) found that large TDR sensors did not measure accurately when the soil was near to saturation, which may have been caused by the variable amount of water in the macropores near to the sensors. Alaoui *et al*. (1997) reported about water content peaks measured by TDR probes after irrigation. These peaks may have reached or exceeded the saturated water content of their soil. Nolz (2013) also found short-lasting peaks of soil–water contents measured by vertically installed frequency-domain and capacitance sensors after irrigation and rainstorm events. These peaks, however, did not perceivably exceed the saturated water content. Similar but longer lasting peaks were measured by a deep vadose-zone monitoring system in cracking clay sediments exposed to dairy waste percolation (Baram *et al*., 2012). Oberdörster *et al*. (2010) found that their horizontally placed TDR probes showed significantly higher peaks of the bulk soil electrical conductivity during infiltration of salt solution into a pre-saturated loamy forest soil, compared with a concurrent electrical resistivity tomography.

Some authors recognize that the measured peaks such as those mentioned previously are indicators of occurrence of preferential flux (Baram *et al*., 2012), while some others regard them as artefacts (e.g. Nolz, 2013). Ireson *et al*. (2006) state that soil–water measurements may be unrealistic due to the interference of instruments with the natural system or other instrumentation artefacts. We suggest that these and similar apparent artefacts can be analysed in order to provide information about the processes of concern. We are not aware of any explicit hydraulic modelling of the effect of gaps and disturbed zones around dielectric soil–water content sensors and the use of this effect for the purpose of sensing preferential flux. Very loosely associated with our problem is the works by Knight *et al*. (1997) and Bore *et al*. (2013), who modelled the electrostatic potential around TDR probes and the effect of fluid-filled or air-filled gaps on their reading.

The objective of this paper is to explore the feasibility of quantifying the rapid downward percolation fluxes in the soil, based on short-lasting peaks of soil–water content measured with large horizontal TDR sensors. We build on the results obtained by Doležal *et al*. (2012a,b; 2015) and on their conceptual model of a thin annular macroporous zone around the sensors, in which the percolating water accumulates for a while. In particular, we want to find out whether or not

a. the high and short-lasting peaks obtained by large horizontal TDR water content sensors and the processes that these data represent can be feasibly simulated by a suitable soil–water model;
b. the model parameters needed for such simulation can be reasonably well estimated, and, once they have been estimated,
c. the simulations can predict rapid percolation fluxes at particular depths from the known rain intensities.

MATERIALS AND METHODS

Site description

The field research was conducted in Prague – Suchdol (50°8'N, 14°23'E, 286 m a.s.l.). Average annual temperature and precipitation are 9.1 °C and 495 mm, respectively (Černý *et al*., 2012). According to Němeček (2009,

personal communication), the soil is Udic Haplustoll (Soil Survey Staff, 1999) or Haplic Chernozem (IUSS Working Group WRB, 2006) of loamy texture on an aeolic loessial substrate. There is virtually no textural difference between topsoil and subsoil. The boundary between the A and C horizons lies at about 35 cm. The transitional A/C horizon is only about 10 cm thick. The layer between about 15 and 25 cm of depth, comprising the lower part of topsoil and the plough sole, is perceptibly more compacted than the rest of the profile. The fine earth contains 22–32.5% sand, 39.5–54% silt and 22–28% clay, while the saturated hydraulic conductivity (100 cm^3 cores) varies roughly between 6×10^{-4} and 4×10^{-1} $cm\,min^{-1}$, and the total porosity varies between 0.40 (plough sole) and 0.54 (topsoil) $cm^3\,cm^{-3}$, its mean value (0–100 cm) being 0.457 $cm^3\,cm^{-3}$. The topsoil dry matter contains about 2.5% of total organic carbon (Nedvěd *et al*., 2008) and 7.8% of calcium carbonate (Brodský *et al*., 2011). No groundwater (i.e. a permanently saturated zone) exists either in the soil profile or in the underlying loess down to at least few metres. The soil has a moderate capacity to swell and shrink. During dry spells, cracks of about 1 to 3 mm wide appear at the surface, lying 15 to 20 cm apart. The structure is granular in the A-horizon and subpolyhedric in the loessial C-horizon. At the higher level of organization, the structure is prismatic. The average water retention curve obtained from 100 cm^3 cores can be approximated, e.g. by the single-porosity (van Genuchten, 1980) equation with the saturated water content $\theta_s=0.475$, the residual water content $\theta_r=0.001$, the capillary rise parameter $\alpha=0.06548\,cm^{-1}$ and the shape factor $n=1.11534$. The soil had been ploughed for several centuries. Grass was sown in spring of 2009 and is maintained since then as a short lawn. The site is neither irrigated nor tile-drained. The grass often suffers from water stress. The terrain is flat. Local short-term ponding of water can be very rarely observed on the surface during very intensive rainstorms.

Field measurement

Precipitation was observed directly on the site at hourly intervals, using a tipping-bucket rain gauge. Three water-content sensors AQUA-TEL-TDR (McCrometer CONNECT, J & S Instruments, Inc., 2010) were installed at 10, 20 and 30 cm depth into horizontal boreholes, predrilled into the vertical wall of a temporary installation pit. The soil above the sensors remained undisturbed. The readings were recorded hourly. The sensors are cylindrical, about 700 mm long, with a 20-mm diameter, locally up to 25 mm. The sensing TDR elements, 457 mm long, and the associated electronics are encapsulated within the sensor body. The diameters of the boreholes (25–27 mm) were slightly larger than those of the sensors; otherwise, the sensors could not get in because of friction. The sensors were wrapped with slurry made of native soil and water before their insertion in the boreholes. The slurry had a very soft plastic consistency just below the liquid limit. Subsequent measurements showed that the slurry came rather quickly (within less than 1 month) into hydraulic equilibrium with the surrounding soil. The slurry did not refill the gaps around the sensors perfectly, which gave rise to a system of artificial macropores surrounding each sensor and connected with the macropores of the natural soil. The existence of these artificial macropores was confirmed by visual inspection during other sensors' de-installation (Figure 1).

The AQUA-TEL-TDR sensors appeared suitable because of their robustness and large length, allowing the measurement of average soil–water contents over relatively large volumes. Doležal *et al*. (2012b) found that they are sensitive to water up to 10 to 50 mm from their surface. The larger range has been observed in a moist soil. Within this range, the sensors are most sensitive to

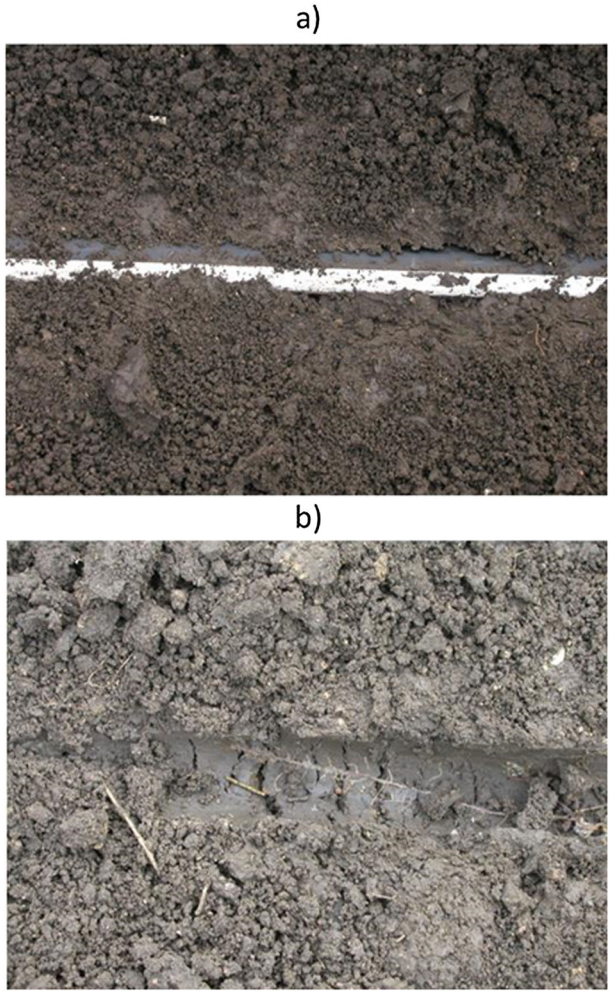

Figure 1. Artificial macropores in the soil around the AQUA-TEL-TDR (time-domain reflectometry) sensors, seen before (a) and after (b) the sensor removal

water when the latter occurs immediately at their surface. Obviously, when there is no such water, they are sensing the water in the soil, both in the thin slurry envelope and also in the native soil around it. As the slurry did not fill the gaps around different sensors in the same way, the readings of the sensors (expressed in $cm^3\,cm^{-3}$) were biassed with respect to each other (Doležal *et al.*, 2012b). This bias was mainly due to installation and seems to be a widespread phenomenon. It is usually eliminated by individual calibration (Ireson *et al.*, 2006).

In our case, the field calibration (Doležal *et al.*, 2012b; 2015) consisted in relating the sensor readings in $cm^3\,cm^{-3}$ to the soil–water contents obtained gravimetrically at a distance of the order of 1 m from the sensors. While the laboratory calibration of another AQUA-TEL-TDR sensor in quartz sand with volumetric water contents from zero to $0.41\,cm^3\,cm^{-3}$ (Doležal *et al.*, 2012b) resulted in a virtually linear calibration equation with a slope (sampling *vs* TDR) 0.654 and no anomalies ($R^2 = 0.992$), the field calibration in our loamy soil showed virtually no correlation between the sampled and TDR values related to individual sensors (with R^2 less than 0.042 and the regression coefficients between −0.267 and −0.002), because of the small-scale heterogeneity of the native soil–water content, captured by gravimetry but averaged by the large TDR sensors. It was, however, found that the standard deviation of water contents obtained by field sampling at a particular depth on different dates was not significantly different from that of the parallel TDR readings (Doležal *et al.*, 2012b). Therefore, it seemed most adequate to relate the water contents derived from field samples to the TDR measurements by applying sensor-specific offset corrections (differences of means) only. The outlying data points affected by aftermaths of rapid percolation events were excluded from the calculation of offsets. The purpose of the field calibration was to make the TDR data from different depths more comparable and to add more physical significance (in terms of the native soil–water content) to the data not belonging to the rapid percolation events. The adding of the offset reduced the effect of the gap between the native soil and the sensors (as did the use of the slurry) whenever the gap was filled with air, but not when it was filled with water. The anomalously high TDR readings obtained during the percolation events of course remained anomalous even after the offset correction. A more detailed description of the experimental area, field measurements and sensor calibration procedures was provided by Doležal *et al.* (2012a,b; 2015).

Modelling

The expected preferential water flow during percolation events was simulated by the HYDRUS 2D/3D (two-dimensional/three-dimensional) software package, version 1.06 (Šimůnek *et al.*, 2012; Šimůnek and van Genuchten, 2008). We chose the dual porosity option, which distinguishes the mobile soil–water domain (macropores) from the immobile one (matrix) and allows for water transfer between them. The model, referred in the succeeding texts to as mobile-immobile or MIM, is based on the mixed formulation of the Richards's equation for the mobile domain, the mass balance for the immobile domain and an equation of the head difference-driven interaction between the two domains, which are, for the two-dimensional case, respectively:

$$\frac{\partial \theta_m}{\partial t} = \frac{\partial}{\partial x}\left[K(h_m)\left(\frac{\partial h_m}{\partial x}\right)\right] + \frac{\partial}{\partial z}\left[K(h_m)\left(\frac{\partial h_m}{\partial z} + 1\right)\right] - S_m - \Gamma_w \tag{1}$$

$$\frac{\partial \theta_{im}}{\partial t} = -S_{im} + \Gamma_w \tag{2}$$

$$\Gamma_w = \alpha_w (h_m - h_{im}) \tag{3}$$

where θ_m and θ_{im} ($cm^3\,cm^{-3}$) are the volumetric water contents in the mobile and the immobile domains, respectively, h_m and h_{im} (cm) are the corresponding pressure heads, K ($cm\,min^{-1}$) is the hydraulic conductivity of the soil (of the mobile domain), t (min) is the time, x (cm) is the horizontal coordinate, z (cm) is the vertical coordinate, positive upwards (cm), S_m and S_{im} (min^{-1}) are the corresponding sink terms (not considered in this study), Γ_w (min^{-1}) is the volumetric rate of water transfer from the mobile domain to the immobile one and α_w ($cm^{-1}\,min^{-1}$) is the first-order mass transfer coefficient. We chose the pressure head-driven inter-domain transfer Equation (3), rather than the fluid saturation-driven one (Šimůnek *et al.*, 2003), because it is the pressure head difference that acts as the actual driving force and because this option allows to optimize the retention curves of the two domains independently, while the use of a water-content-difference analogue of (3) in HYDRUS 2D/3D would require that water retention properties of the matrix and the preferential flow domain be identical (Šimůnek *et al.*, 2012).

The retention curves of the two domains were approximated by the usual van Genuchten (1980) formulae. The total soil–water content was taken as the sum of the two domains' water contents:

$$\theta = \theta_m + \theta_{im} \;\; ; \quad \theta_r = \theta_{r,m} + \theta_{r,im} \;\; ; \quad \theta_s = \theta_{s,m} + \theta_{s,im} \tag{4}$$

where θ ($cm^3\,cm^{-3}$) is the total soil–water content, $\theta_{r,m}$, $\theta_{r,im}$ and θ_r ($cm^3\,cm^{-3}$) are the residual water contents of the mobile domain, the immobile domain and the soil as a whole, respectively, and $\theta_{s,m}$, $\theta_{s,im}$ and θ_s ($cm^3\,cm^{-3}$) are analogous symbols for the saturated water contents. The hydraulic conductivity K is a function of the mobile domain pressure head h_m according to the Mualem–van Genuchten

formula (van Genuchten, 1980). The total soil–water flux is assumed to be equal to the preferential flux.

Our choice of model was a compromise between the need for physical adequacy, the requirement of parsimony in the number of parameters and the ease of relying on at least some standard soil physical properties measured in the laboratory, namely, the retention curves and the saturated hydraulic conductivities. A consequence of this choice was that only the rapid soil–water movement could be simulated, while the slower movement taking place within the soil matrix and avoiding the macropores (evaporation, capillary rise and redistribution) had to be put aside, because the model did not allow for water movement in the matrix.

For contrast, as instigated by a reviewer, we tried to use the Durner equilibrium dual porosity model (Durner, 1994; Šimůnek *et al.*, 2012), also supported by HYDRUS 2D/3D. In the Durner model, the flow and retention of water in the soil are described by a single Richards's equation without any mass-transfer term:

$$\frac{\partial\theta}{\partial t}=\frac{\partial}{\partial x}\left[K(h)\left(\frac{\partial h}{\partial x}\right)\right]+\frac{\partial}{\partial z}\left[K(h)\left(\frac{\partial h}{\partial z}+1\right)\right]-S \quad (5)$$

$$\theta=\theta_r+(\theta_s-\theta_r)S_e \quad (6)$$

$$S_e=S_{e1}+S_{e2}=w_1[1+(\alpha_1 h)^{n_1}]^{-m_1}+w_2[1+(\alpha_2 h)^{n_2}]^{-m_2} \quad (7)$$

$$w_1+w_2=1 \quad (8)$$

where θ ($cm^3\,cm^{-3}$) is the total volumetric water content, h (cm) is the pressure head (the same in both pore domains), S_e is the total relative soil–water content, K_s is the saturated hydraulic conductivity ($cm\,min^{-1}$) and, for $i=1$ or 2 (denoting the two pore domains in local equilibrium), S_{ei} is the relative soil–water contents, w_i is the volumetric weighting factors, α_i, n_i and $m_i=1\text{-}1/n_i$ are the van Genuchten parameters and S is the sink term (not considered).

Other modelling options, not tested in this study, include in particular the dual permeability model with a Richards's equation in either of the domains (e.g. Šimůnek *et al.*, 2003) and kinematic wave models for the preferential flow domain (e.g. Alaoui *et al.*, 2003; Jarvis and Larsbo, 2012). As far as we know, no commonly available model allows to combine various modelling options (e.g. one option in one material and another option in the other material) within a single model run.

A 2D model was needed in order to realistically simulate the concentration of flow and the temporary accumulation of water around the sensors. The 2D flow simulation region was obtained by projecting the 3D prototype onto a vertical plane perpendicular to the sensors. It was defined as a vertical rectangle 100 × 75 cm (depth × width), containing three impermeable circular features (2 cm in diameter) that represented the cross sections of the TDR probes, with their centres at 10, 20 and 30 cm depths and at 12.5, 37.5 and 62.5 cm horizontal distance from the left boundary of the flow region (Figure 2). An annular zone 0.25 cm thick was defined around each TDR sensor to represent the average behaviour of the slurry material, including its macropores, over the sensor's entire active length (457 mm). While it

$$K(S_e)=K_s\frac{(w_1S_{e1}+w_2S_{e2})^l\left(w_1\alpha_1\left[1-\left(1-S_{e1}^{1/m_1}\right)^{m_1}\right]+w_2\alpha_2\left[1-\left(1-S_{e2}^{1/m_2}\right)^{m_2}\right]\right)^2}{w_1\alpha_1+w_2\alpha_2} \quad (9)$$

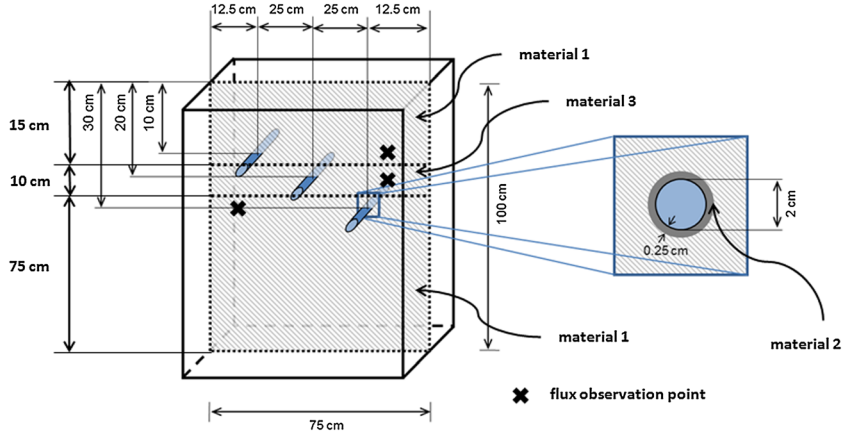

Figure 2. Two-dimensional flow region definition for dual-porosity models. Materials 1 and 3 are the native soil. The dark-shaded annulus in the inset (material 2) is the sensor envelope with special properties (slurry and artificial macropores). The crosses denote the points in which the simulated native soil fluxes are observed

may seem unusual to include artificial macropores around the sensors into the macroscopically continuous and homogeneous annuli, this approximation is completely acceptable, especially when one realizes that the same macroscopically continuous representation is normally used for the macropores of the native soil and, indeed, for any soil pores. No weighting function for expressing the sensitivity of TDR sensors to water contents occurring at different distances from their surfaces was explicitly assumed in the model. Instead, the sensitivity to the native soil–water content (outside the slurry envelope) was taken into account by applying the field calibration equation to the TDR-measured data, and the sensitivity to the slurry envelope water content was taken into account by adjusting the saturated water content of the mobile domain in the material 2 so that it corresponds to TDR measurements during the percolation events. Zero-flux boundary conditions were defined on the sides of the 2D flow region and on the surfaces of the sensors. Free drainage at unit hydraulic gradient was postulated at the bottom of the flow region, while an atmospheric boundary condition was prescribed at the top of it in terms of hourly averaged rainfall rate data. No surface ponding occurred during the simulations.

The onset of rainfall in each simulation run took place after a 120-min pre-rain period. Two typical measured percolation events were mimicked by simulations. The former was instigated by a series or rainstorms from 23 July 2010, 01:00 (24-h format) to 24 July 2010, 09:00, with the total 42.2 mm. The latter was due to a series of less-intensive rains from 16 November 2010, 04:00 to 20 November 2010, 00:00, with the total 10.7 mm. The duration of each simulated period was 7080 min. The constant pressure head (−1100 cm for the July event and −250 cm for the November event) initial condition was used in both domains. This pressure head corresponded approximately to the geometric mean of the pressure heads obtained from the pre-event TDR-measured soil–water contents at the three depths. The latter was converted to pressure heads by using the sum of the van Genuchten – parameterized retention curves for the mobile and the immobile domains of the slurry annuli. This is hoped to be a suitable and virtually universal procedure for estimation of initial conditions for similar simulations.

The finite element grid of the 2D flow region was composed of 9593 nodes, 18 742 2D triangular elements and 994 one-dimensional elements of boundaries and internal lines. The grid was sufficiently refined around each TDR probe (Figure 3). The simulated soil–water contents to be compared with the TDR-measured values were obtained as arithmetic means of the simulated values in 64 observations points, creating a circle around each sensor at 0.1 cm distance from the sensor surface. It was found by numerical analysis (not shown) that the exact

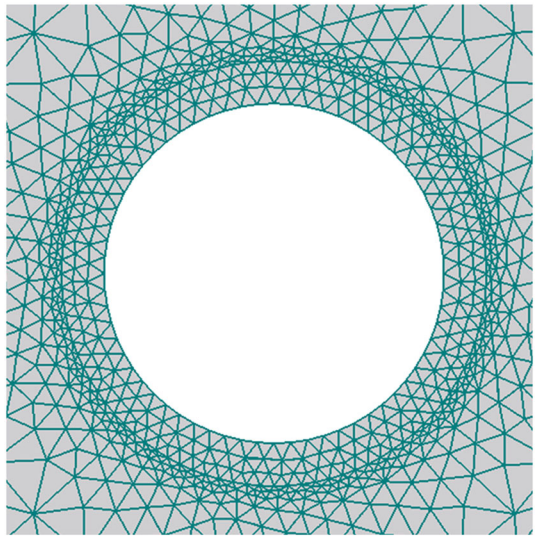

Figure 3. A detail of the two-dimensional finite element grid for the dual porosity model in the vicinity of a time-domain reflectometry (TDR) sensor. The slurry envelope is represented by the innermost four layers of nodes (including the layer lying at the very surface of the sensor). The observation points make the second layer (counted from the sensor surface)

distance of the observation points from the sensor surface was not critical, because there was only a little difference between simulated water contents at different finite element nodes within a particular slurry annulus at any particular time. For the same reason, the choice of the slurry annulus thickness was not critical. The water contents and the vertical fluxes in the native soil (the latter being the final goal of the simulation), were taken from typical single nodes at 10, 20 and 30 cm depths at sufficient horizontal distances from the sensors (at 69.1, 69.4 and 11.9 cm from the left boundary of the region, respectively) and therefore virtually unaffected by their presence, as checked by comparing water contents at various distances from the sensors (not shown). Similarly located nodes at 12, 27 and 35 cm depths were used for obtaining simulated fluxes to compare with water balance in Table IV.

Three soil materials were defined within the flow region. The first material represented jointly the native topsoil (0–15 cm) and subsoil (25–100 cm). The second material symbolized the slurry annuli around the sensors, while the third one corresponded to the layer of increased compaction at 15–25 cm. The allocation of materials and the initial estimates of their immobile domain parameters were inspired by measured profiles of soil texture and hydraulic properties. In particular, the retention curves (taken as appropriate to characterize the immobile domain) and the saturated hydraulic conductivities (used as initial estimates of K_s for the native soil materials) were taken into account. Some parameters were then optimized for the July percolation event, while the November event was used for validation. The inverse simulation option of

HYDRUS was used at some stages, followed by a trial-and-error optimization. The saturated water contents of the preferential flow domains of the native soil were deliberately kept very low to simulate the low volume of macropores. The analogous parameter for the slurry layer was set high, to allow for both the higher volume of macropores in the slurry layer and the increased sensitivity of the TDR probes with respect to water in their vicinity. Its value was adjusted by trial and error so that the maximum total water contents obtained by simulation become similar to the measured ones. The residual water contents of the preferential flow domains were set *a priori* to zero and were not optimized, because the measured data did not provide enough information about the dry part of the water content range. The only parameters optimized for the three materials were the saturated hydraulic conductivities and the van Genuchten retention curve shape parameters (α and n) of the preferential flow domains. Care was taken that the unsaturated hydraulic conductivity of the slurry material be higher than that of the other two materials over the range of pressure heads between about -100 cm and zero, so that the capillary barrier effect at the entry of water into the slurry layer is avoided; the slurry annuli served as attractors of the simulated water flow (checked but not shown). It was assumed that the physical disturbances due to soil tillage, compaction and slurry preparation affected mainly the preferential flow domain, while the retention curve parameters of the matrix domain were taken the same for all three materials as obtained from the laboratory measurements. The residual and saturated water contents of the matrix domain were estimated *a priori* and not optimized. The mass transfer coefficients α_w were estimated by trial and error and were kept small in order that the simulated inter-domain mass transfer rates remain realistic everywhere and at all times, as demonstrated in the succeeding texts. The resulting final set of parameters is presented in Table I. Probationary sensitivity analysis indicated that no further improvement of model performance can be easily reached by variation of model parameters.

The parameters for the Durner equilibrium dual porosity model were then derived from the parameters of the MIM non-equilibrium dual porosity model (Table I) as follows:

$$\theta_r = \theta_{r,m} + \theta_{r,im} \;\; ; \quad \theta_s = \theta_{s,m} + \theta_{s,im} \tag{10}$$

$$\alpha_1 = \alpha_m \;\; ; \quad \alpha_2 = \alpha_{im} \;\; ; \quad n_1 = n_m \;\; ; \quad n_2 = n_{im} \tag{11}$$

$$w_2 = \frac{\theta_{s,im} - \theta_{r,im}}{\theta_s - \theta_r} \;\; ; \quad w_1 = 1 - w_2 \tag{12}$$

taking the domain 1 as corresponding to the mobile domain of the MIM model. The remaining parameters K_s and l remained unchanged. In this way, the Durner model was made as similar as possible to the MIM model. Further effort for optimization of the Durner model parameters in order that it better resembles the observations did not lead to a success.

Table I. Optimized van Genuchten parameters of model materials

Material:	1	2	3
Description:	Topsoil and subsoil	Shrunken slurry	Lower topsoil and plough sole
$\theta_{r,m}$	0	0	0
$\theta_{s,m}$	0.03	0.4	0.01
α_m (cm^{-1})	0.010315	0.010315	0.06548
n_m	2	3	1.5
K_s ($cm\,min^{-1}$)	0.18	0.3	0.11
l	0.5	0.5	0.5
$\theta_{r,im}$	0.001	0.001	0.001
$\theta_{s,im}$	0.475	0.475	0.475
α_{im} (cm^{-1})	0.06548	0.06548	0.06548
n_{im}	1.11534	1.11534	1.11534
α_w ($cm^{-1}\,min^{-1}$)	0.00006	0.001	0.00006

The adequacy of simulation was estimated by comparing the simulated and TDR-measured soil–water contents, first qualitatively and then using the mean error (*ME*) and the root mean square error (*RMSE*), both evaluated between time zero (start of simulation) and 7080 min (end of simulation). It was also tested to which extent the simulation outputs fulfil the soil–water balance over the percolation event (according to Pirastru and Niedda (2010)):

$$D = \left(\theta_j - \theta_{j+1}\right)\Delta z + R \tag{13}$$

where D is the percolation flux at the depth Δz, θ_j is the mean soil–water content of the layer between the soil surface and the depth Δz before the event, θ_{j+1} is the same after the event and R is the precipitation total over the event. The evapotranspiration was neglected. It was assumed that the TDR-measured soil–water contents (corrected by the field calibration) before the percolation event can be regarded as virtually unbiassed. The analogous measurement taken after the percolation event (yet within the range of the period simulated) can also be taken as almost unbiassed, with a reservation that some water having flowed through the macropores during the event may have been absorbed by the matrix and so may have contributed to the after-event total soil–water content. We calculated D from the measured data and compared it with the time integral of the simulated fluxes over the same period at the depths corresponding to bottoms of the balanced layers. As the simulated data at the sharp boundaries between different materials (at depths 15 and 25 cm) were to some extent affected by numerical noise, we chose to do the balance for slightly different depths,

namely, 12 and 27 cm, respectively. The bottom of the third layer was kept at 35 cm depth, as there was no boundary between different materials there. The mean soil–water contents θ_j and θ_{j+1} in (13) were calculated as weighted means of TDR measurements made within particular layers (0–12, 0–27 and 0–35 cm), the weights being taken as the thicknesses of the corresponding sublayers (12, 15 and 8 cm for the TDR measurements at 10, 20 and 30 cm, respectively).

RESULTS AND DISCUSSION

Figures 4 and 5 show the MIM model simulations of soil–water contents before, during and after two percolation events in the nodes near the sensors (in the zones of the slurry annuli at 0.1 mm distance from the sensors' surface, averaged along the entire circumference of the sensors). These simulated data are compared with those measured by the sensors over the same periods and corrected by field calibration. The July 2010 event is a calibration period, and the November 2010 event is a validation period. Qualitatively judged, the measured data are reasonably well approximated by the simulations at 10 cm for both periods and at 30 cm for the November period. The agreement between simulation and measurement is moderately good at 30 cm for the July period, but poor at 20 cm for both periods. The simulated values at all depths tend to be systematically higher than the measured ones, except for November at 30 cm. Table II presents basic statistical indicators of agreement between the MIM simulation and the measurement. The overall pattern of model performance according to *RMSE* corresponds approximately to the visual assessment, except that *RMSE* renders the agreement less satisfactory at 10 cm and more satisfactory at 30 cm for both periods.

The overall performance according to *RMSE* is even slightly better in November than in July. Poor performance at 20 cm is confirmed by both *RMSE* and *ME*. The negative *ME* at 30 cm in November indicates that the simulated values are on average smaller than the measured ones. The lack of substantial difference in overall simulation performance between July and November suggests that the soil properties and parameters may not have changed between July and November 2010. The performance of the model can be regarded as qualitatively adequate, i.e. the model can simulate the basic features of the measurement in a qualitative, but not yet quantitative way. The persisting discrepancies confirm that it is rather difficult to optimize the soil parameters of the model for such a complex flow region, based on existing measurements.

Figures 4 and 5 also show simulated water contents in the native soil far from the slurry annuli. In spite of the absence of independent direct measurements of these water contents, we can make a qualitative conclusion that the native soil water content varies much less than the

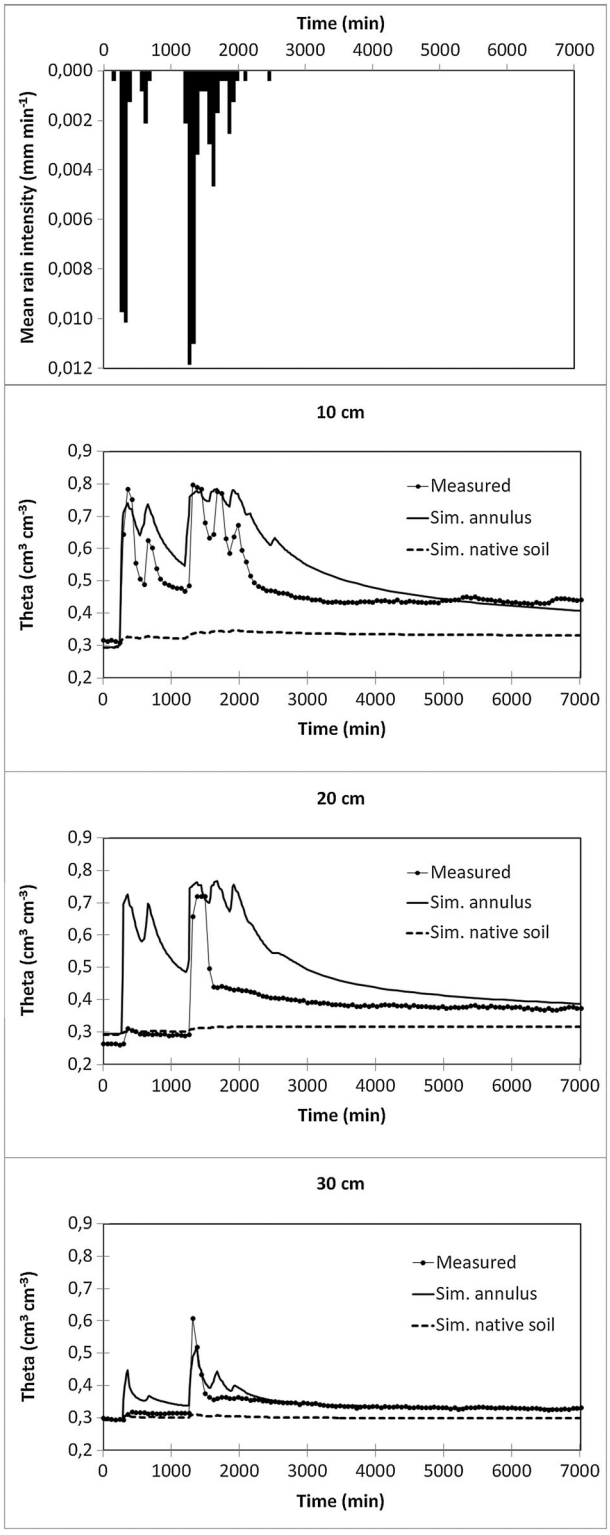

Figure 4. Comparing the results of two-dimensional mobile-immobile (MIM) dual-porosity simulation in terms of soil–water contents with the time-domain reflectometry (TDR) measurements, July 2010 (calibration event)

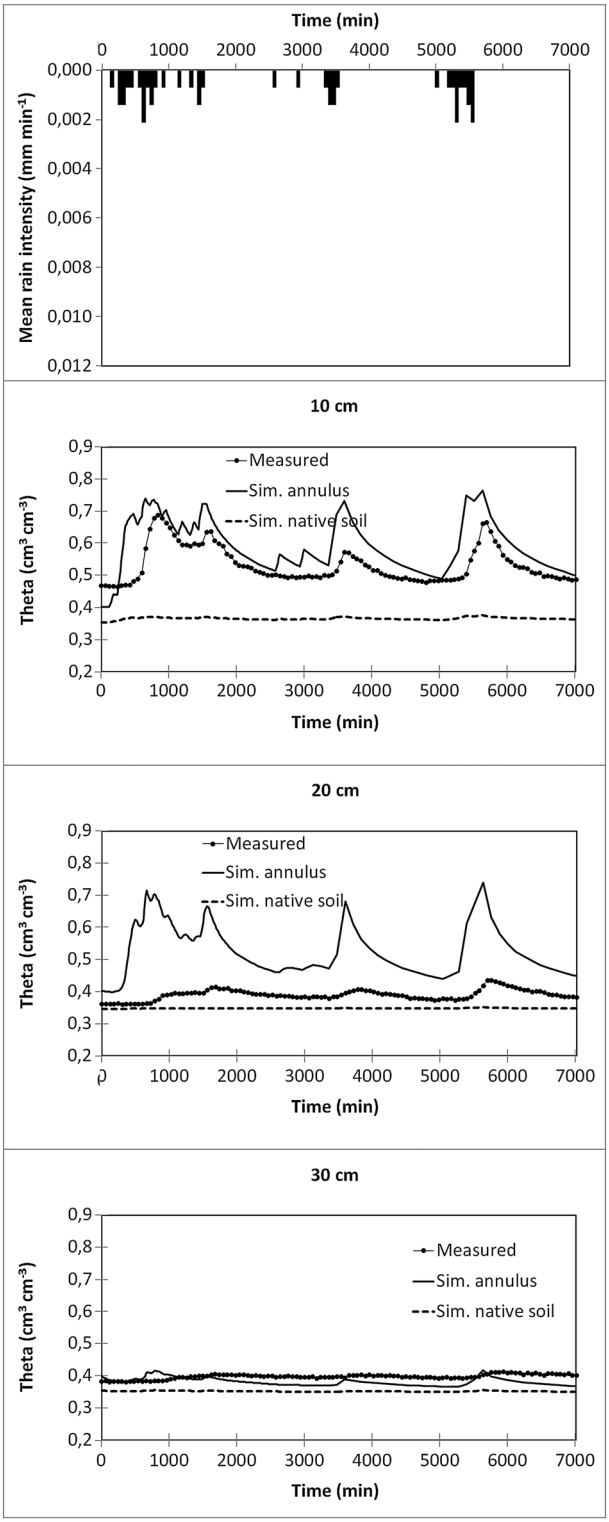

Figure 5. Comparing the results of two-dimensional mobile-immobile (MIM) dual-porosity simulation in terms of soil–water contents with the time-domain reflectometry (TDR) measurements, November 2010 (validation event)

TDR readings. Figures 6 and 7 present simulation results of the Durner equilibrium dual porosity model for the same two events. We may conclude that the Durner model with the soil hydraulic properties similar to those of the MIM model behaves substantially differently. It predicts that the water passing through the soil is largely absorbed by the soil matrix as long as the matrix is unsaturated. Consequently, the water percolation is little or none unless the matrix becomes saturated enough. After that, the percolations becomes quick, but the water content of the soil then remains high for a long time because of slow drainage of the matrix. The simulated water content hydrographs for the slurry annular zones are substantially different from the TDR-measured ones. On the other hand, the Durner model suggests that not only the slurry annuli but also the native soil responds to precipitation with considerable water content amplitudes, which is especially visible during the July event (Figure 6). Table III presents statistical indices (*RMSE* and *ME*) illustrating that the performance of the Durner model is generally poor, except perhaps for November at 30 cm. Our attempts to further optimize the soil hydraulic parameters of the Durner model led us to a conclusion that the only way how to make the simulated water content hydrographs more alike to the measured ones, with their rapid ascents and almost equally rapid descents, would be to keep the saturated water content parameter (θ_s) of the native soil very low, about 0.01 to 0.1, which is, of course, unrealistic. Even then, the Durner model would not yield satisfactory results (not shown).

Table II. Statistical indices of the non-equilibrium [mobile-immobile (MIM)] dual-porosity model performance [mean error (*ME*, simulated–measured) and root mean square error (*RMSE*)]

	ME ($cm^3\,cm^{-3}$) for the depth			*RMSE* ($cm^3\,cm^{-3}$) for the depth		
Event	10 cm	20 cm	30 cm	10 cm	20 cm	30 cm
July	0.0485	0.1097	0.0090	0.0829	0.1559	0.0260
November	0.0578	0.1348	−0.0171	0.0794	0.1540	0.0231

The same simulation runs also provided estimates of vertical soil water flux hydrographs in the native soil far enough from the sensors (Figure 8 for the MIM model and Figure 9 for the Durner model). The fluxes were compared with the water balance estimates according to (13) in Table IV and with the precipitation rates in Figures 8 and 9. Leaving aside the first few hours of the July event, when the soil is being rewetted, Figure 8 suggests that the rain intensities of the order of $10^{-2}\,cm\,min^{-1}$, which occurred during the highest hyetograph peaks in July, are not perceivably higher than the soil water flux peaks occurring as a result of them at 10, 20 and 30 cm. This happens because the mobile water domain is, at these moments, almost saturated and quickly transmits water down the soil profile. Hence, the presence

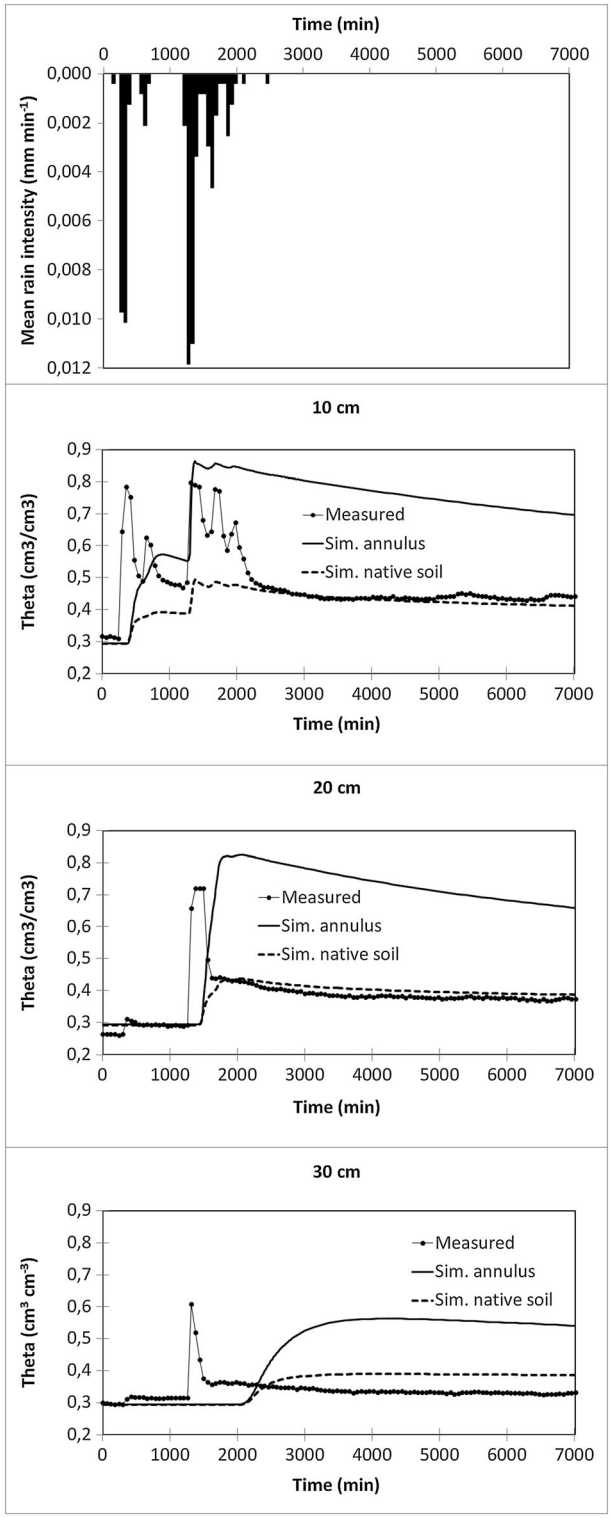

Figure 6. Comparing the results of two-dimensional Durner equilibrium dual-porosity simulation in terms of soil–water contents with the time-domain reflectometry (TDR) measurements, July 2010 (calibration event)

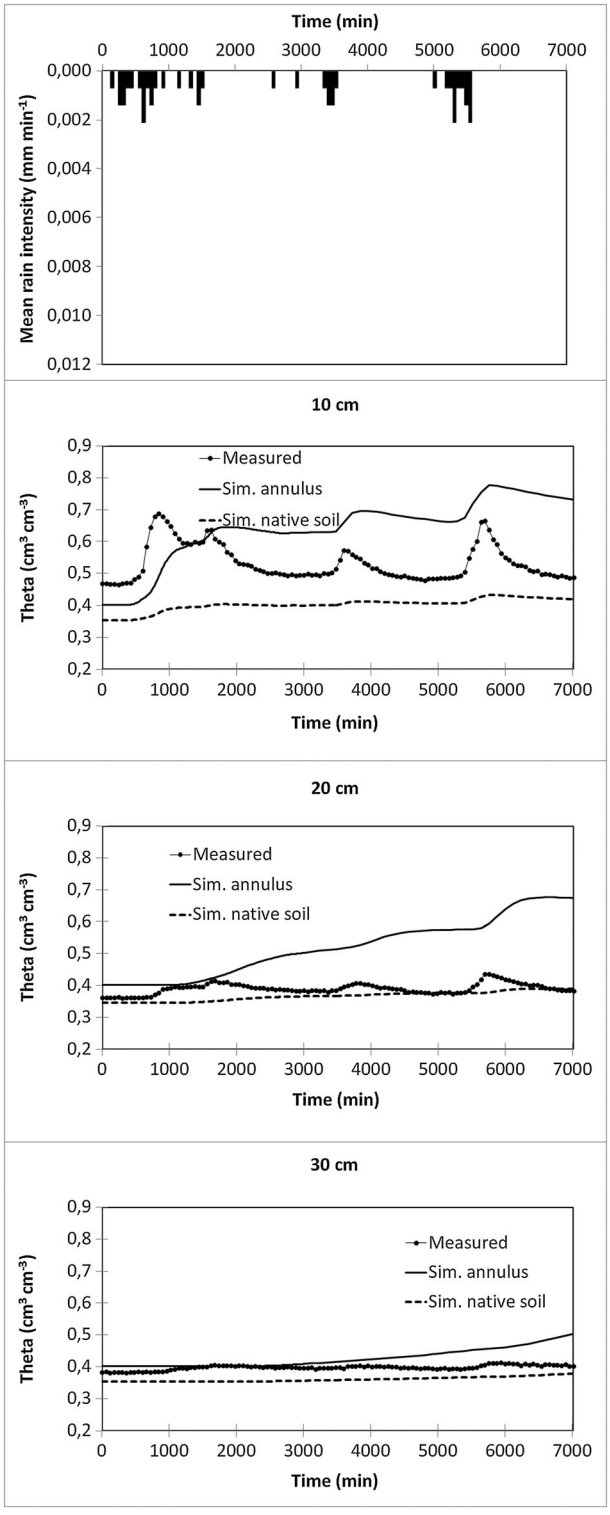

Figure 7. Comparing the results of two-dimensional Durner equilibrium dual-porosity simulation in terms of soil–water contents with the time-domain reflectometry (TDR) measurements, November 2010 (validation event)

of permeable macropores renders the rapid percolation of water and pollutants well possible even in a Chernozem soil under a moderately dry climate.

A different picture can be seen in July during the secondary showers and in November. In these cases, the peak rain intensities are by almost an order of magnitude

Table III. Statistical indices of the equilibrium (Durner) dual-porosity model performance [mean error (*ME*, simulated–measured) and root mean square error (*RMSE*)]

	ME ($cm^3\,cm^{-3}$) for the depth			*RMSE* ($cm^3\,cm^{-3}$) for the depth		
Event	10 cm	20 cm	30 cm	10 cm	20 cm	30 cm
July	0.2281	0.2551	0.1219	0.2815	0.3140	0.1772
November	0.1083	0.1306	0.0294	0.1580	0.1568	0.0396

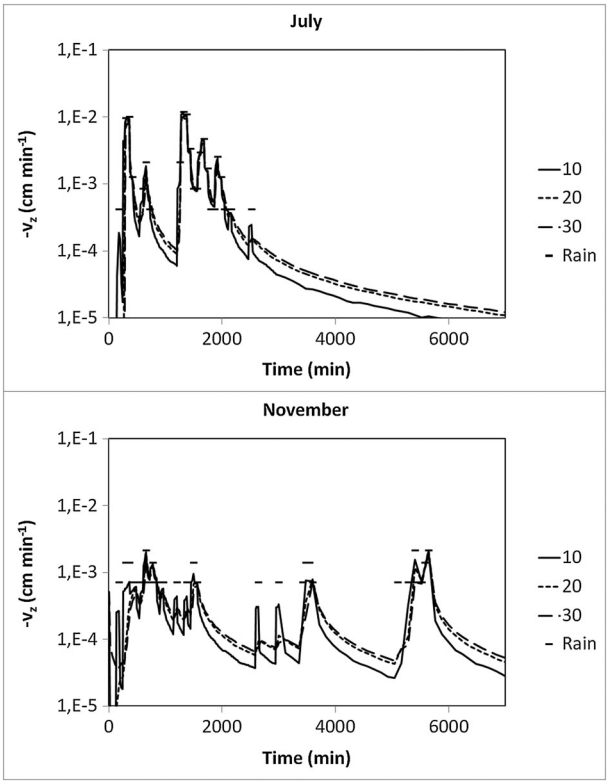

Figure 8. Vertical soil–water fluxes, simulated by the mobile-immobile (MIM) model, for (a) June event and (b) November event. Average hourly rainfall rates are plotted as points for comparison

lower than those during the highest hyetograph peaks of July. Then, the peak soil water fluxes at 10 cm are distinctly lower than the corresponding peak rain intensities but markedly higher than the soil water fluxes at larger depth, which react only a little or not at all to these rains. Even in these cases, however, the reaction of soil water flux at any depth comes almost simultaneously with the rain or after only a little delay, not exceeding 1 h. A similar rapid reaction to precipitation was reported, for example, by Pirastru and Niedda (2010) for the fissured chalk rock, in the cases when the rock was wet. According to Figure 8, the fluxes at all depths gradually decline during rainless periods, whereas the fluxes at larger depths decline more slowly than those at smaller

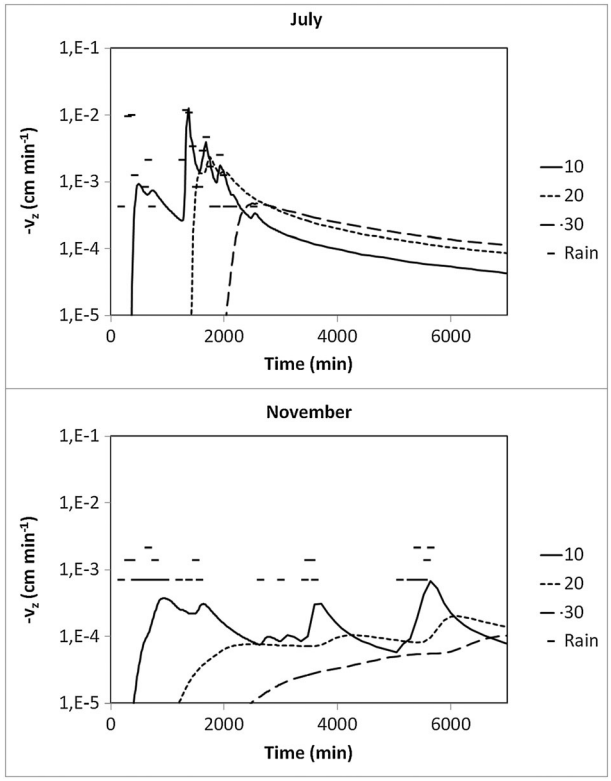

Figure 9. Vertical soil–water fluxes, simulated by the Durner model for (a) June event and (b) November event. Average hourly rainfall rates are plotted as points for comparison

Table IV. Percolation fluxes derived by water balance from the measured soil–water contents and rainfall sums (according to Pirastru and Niedda, 2010), compared with the vertical fluxes simulated by the non-equilibrium (MIM) and the equilibrium (Durner) dual porosity models

Event		July	November
Length of period (min)		3720	7080
Cumulative rainfall (cm)		4.22	1.78
Cumulative vertical flux (cm) at the depth:			
12 cm	measured	2.84	1.73
	MIM	3.75	1.79
	Durner	2.63	0.98
27 cm	measured	1.10	1.62
	MIM	3.55	1.77
	Durner	0.89	0.33
35 cm	measured	0.85	1.48
	MIM	3.37	1.71
	Durner	0.17	0.13

MIM, mobile-immobile.

depths. The fluxes at larger depths go on declining even when the short-lasting low-intensity showers (e.g. in July at 2100 min) produce secondary peak fluxes at small depths, which even may not exceed the slowly declining fluxes at larger depths. Analogous flux hydrographs

obtained by the Durner model (Figure 9) show a comparably quick rise of flux only in the hours when the rain intensities were very high and the soil matrix was near to saturation. The quick rise of flux is, however, followed by a slow decline of the same. This observation only confirms our conclusion that the Durner model is not suitable.

Table IV compares the measured cumulative fluxes obtained by water balance (13) according to Pirastru and Niedda (2010) with the cumulative rainfall and the cumulative percolation fluxes simulated by the non-equilibrium (MIM) and the equilibrium (Durner) models. The measured and simulated fluxes are of the same order of magnitude. In June, the Durner model agrees better with the water balance method than the MIM model (except for 35 cm), while in November, the MIM model performs better. In general, the MIM model underestimates the dampening of the flux with depth, and the Durner model overestimates it.

When discussing the choice of the model and its parameterization, we must reiterate that our decision to use a simpler dual porosity model, with one of the flow domains immobile, rather than the dual permeability model with both domains mobile (Šimůnek *et al*., 2003; Šimůnek and van Genuchten, 2008) ended with a set of parameters (Table I) suitable for describing short percolation events only. With our parameterization, a major part of soil water is regarded as virtually immobile, and it is only in the thin annuli around the sensors that the model allows substantial amounts of mobile water to accumulate for a short time. This seems to correspond to reality, i.e. the water modelled as immobile is even in reality slow to move on the time scale of a percolation event. Neglecting evapotranspiration (of the order of magnitude of mm d^{-1}) may have caused about 10% overestimation of the upper boundary condition, which is of the order of magnitude of tens of mm d^{-1}, but this has been qualitatively counterbalanced by the generally known tendency of standard rain gauges to underestimate precipitation (e.g. Wagner, 2009). The adoption of this model also brings about a necessity to estimate a new initial condition for each event, based on the direct pre-event TDR measurements, using, e.g. the procedure described previously.

The inter-domain transfer coefficients α_w for the native soil (materials 1 and 3 in Table I) are quite small, in contrast to that for the slurry annuli. They are about ten to hundred times smaller than the typical values obtained by Köhne *et al*. (2004) (their ω^* in their Table IV), for a loamy soil in Northern Germany, which is lighter than our soil. We deliberately kept these inter-domain transfer coefficients low during the optimization, in an effort to avoid unrealistically high inter-domain transfer rates Γ_w approaching 1 min^{-1}. Finally, it appeared that even for the slurry annuli (material 2), where our transfer coefficient was of the same order of magnitude as those of Köhne *et al*. (2004), our MIM simulation of the June event produced reasonable maximum Γ_w values around the 10 cm sensor at 300 min, when the immobile water content rose by 0.017 over 15 min. However, our attempts at improving the performance of the MIM model further by enhancing the inter-domain transfer coefficients were not successful.

CONCLUSIONS

Our results suggest that water content measurements made with several large dielectric (e.g. TDR) sensors at different depths and accompanied by precipitation measurements may indeed yield insight into the temporal and spatial patterns of rapid soil water fluxes, provided that the model of soil water movement is adequately set, and its parameters, expressing the properties of a particular soil profile and its interaction with a particular assembly of sensors, have been adequately estimated.

The anomalous and short-lasting water content peaks measured by Doležal *et al*. (2012a,b; 2015), especially if they are higher than the saturated water content of the native soil, are rather reliable qualitative indicators of the rapid downward percolation, which is very probably of preferential (i.e. non-equilibrium) nature. This is evidenced by the fast response of water content peaks to rain or snowmelt inputs, an almost equally rapid response to the cessation of the inputs, and by fact that the non-equilibrium (MIM) dual porosity model, even though not yet able to simulate the reality perfectly, yields better results (in terms of water content and flux density *vs* time) than the equilibrium Durner dual porosity model.

The optimization of soil parameters and other model settings appeared to be quite difficult. More sophisticated optimization procedures, involving additional input information such as water balance, may be needed. In spite of these difficulties, the existing set of parameters of the non-equilibrium model made it possible to investigate and partly explain how systems of this type work. In particular, the model is capable of predicting, even if not yet accurately, the anomalous water content readings during rapid percolation events and the attenuation of rain impulses along the percolation paths (the attenuation being underestimated). At this stage of research, we consider it appropriate to expose our approach to public discussion.

Our study confirms that these or similar sets of water content sensors can be used for detection of rapid percolation fluxes and suggests that, after some additional effort, quantitative measurements of these percolation fluxes may be possible. In our study, we used the water

content sensors, in the first place, for the estimation of model parameters and for validation of the model. Their readings were also needed to estimate the initial conditions for particular simulation runs. On the other hand, the flux hydrographs were not directly derived from the readings of water content sensors. Instead, they were derived from model simulations in which the precipitation measurements were used as inputs.

Using slurry during the installation of large sensors (which is a widely recommended procedure, Sentek, 2003; J & S Instruments, Inc., 2010; Aquacheck, 2013) may make their readings during percolation events (especially in the case of horizontally installed sensors) of little direct use, while the readings outside the percolation events are useful but should be corrected based on a sort of field calibration that comprises the effect of the slurry and the gap. On the other hand, this apparent disadvantage turns out to be also an advantage, making these sensors a sort of amplifiers of the preferential flux signals. The observations by Baram *et al*. (2012) or Nolz (2013) suggest that unexpected peak readings, not necessarily anomalously high, of other types of water content sensors may in principle also be used to infer about the magnitude of preferential flux. In these cases, however, the effect may not be as strong as in the case of large horizontal sensors.

The practical importance of this research is manifold. First, it helps us to interpret more fully the soil water content measurement, including some features regarded up to now as biassed due to artefacts. Second, it suggests a method of estimating soil water flux hydrographs at different depths and, thereby, the rates of groundwater recharge and the risk of groundwater pollution. Third, as already mentioned by Doležal *et al*. (2012a), this methodology enables irrigation practitioners to use their soil water metres in a better way, avoiding misinterpretation of anomalous peaks.

ACKNOWLEDGEMENTS

This study was supported by the MOEL-Plus-Förderungsprogramm of the Austrian Research Association (ÖFG) and the research programme MSM6046070901 'Sustainable agriculture, quality of products, sustainable use of natural and landscape resources' (2005–2011, MSM) of the Czech University of Life Sciences in Prague, financed by Ministry of Education, Youth and Sports of the Czech Republic. The collaboration was further supported by the University Exchange Program AKTION between the Republic of Austria and the Czech Republic, projects 64p12 PREFLOWAT, 67p10 PREFLOWAT2 and 70p6 PREFLOWAT3. Soil properties were taken from the M.Sc. theses by Helena Kozáková (1994) and Petra Krkavcová (2010). Some precipitation data were provided by the Institute of Atmospheric Physics of the Academy of Sciences in Prague. Software for data post-processing was written by Wolfgang Sokol from BOKU. Valuable comments by anonymous reviewers and Dr. Marek Rodný from the Institute of Hydrology in Bratislava are gratefully acknowledged.

REFERENCES

Adamsen FJ, Hunsaker DJ. 2000. Water Content Determination in Saline Soils Using Self-Contained TDR and Electrical Capacitance Systems. In *National Irrigation Symposium, Phoenix, Arizona, USA*, Evans RG, Benham BL, Trooien TP (eds). American Society of Agricultural Engineers: St. Joseph; 351–356.

Alaoui AM, Germann P, Lichner L, Novak V. 1997. Preferential transport of water and 131Iodide in a clay loam assessed with TDR techniques and boundary-layer flow theory. *Hydrology and Earth System Sciences* **1**: 813–822.

Alaoui A, Germann P, Jarvis N, Acutis M. 2003. Dual-porosity and kinematic wave approaches to assess the degree of preferential flow in an unsaturated soil. *Hydrological Sciences Journal* **48**: 455–472. DOI:10.1623/hysj.48.3.455.45289.

Allaire SA, Roulier S, Cessna AJ. 2009. Quantifying preferential flow in soils: a review of different techniques. *Journal of Hydrology* **378**: 179–204. DOI:10.1016/j.jhydrol.2009.08.013.

Aquacheck. 2013. Probe installation. 2. Aqua Check Soil Moisture Management, Perry, Iowa, USA. http://www.aquachecktech.com/assets/installman.pdf, October 27, 2013.

Baram S, Kurtzman D, Dahan O. 2012. Water percolation through a clayey vadose zone. *Journal of Hydrology* **424–425**: 165–171. DOI:10.1016/j.jhydrol.2011.12.040.

Brodský L, Klement A, Penížek V, Kodešová R, Borůvka L. 2011. Building soil spectral library of the Czech soils for quantitative digital soil mapping. *Soil & Water Research* **6**: 165–172.

Beven K, Germann P. 2013. Macropores and water flow in soils revisited. *Water Resources Research* **49**: 3071–3092. DOI:10.1002/wrcr.20156.

Bore T, Placko D, Taillade F, Lesoille-Delepine S, Six G, Sabouroux P. 2013. Theoretical and experimental study of a time-domain-reflectometry (TDR) probe used for water content measurement of clayrock through their electromagnetic properties. *Proc. SPIE* 8692, Sensors and Smart Structures Technologies for Civil, Mechanical, and Aerospace Systems 2013, 86921U (April 19, 2013). DOI: 10.1117/12.2009832.

Černý J, Balík J, Kulhánek M, Vašák F, Peklová L, Sedlář O. 2012. The effect of mineral N fertiliser and sewage sludge on yield and nitrogen efficiency of silage maize. *Plant, Soil and Environment* **58**: 76–83.

Clothier BE, Green SR, Deurer M. 2008. Preferential flow and transport in soil: progress and prognosis. *European Journal of Soil Science* **59**: 2–13. DOI:10.1111/j.1365-2389.2007.00991.x.

Crosbie R, Jolly I, Leaney F, Petheram C, Wohling D. 2010. Review of Australian groundwater recharge studies. Water for a Healthy Country National Research Flagship Series. CSIRO: Canberra; 81. http://www.clw.csiro.au/publications/waterforahealthycountry/2010/wfhc-review-Australian-recharge.pdf, January 7, 2013.

Doležal F, Matula S, Moreira Barradas JM. 2012a. Improved horizontal installation of large soil moisture content sensors and interpretation of their readings in terms of preferential flow. *Journal of Hydrology and Hydromechanics* **60**: 333–338. DOI:10.2478/v10098-012-0029-9.

Doležal F, Matula S, Moreira Barradas JM. 2012b. Percolation in macropores and performance of large time-domain reflectometry sensors. *Plant, Soil and Environment* **58**: 503–507.

Doležal F, Matula S, Moreira Barradas JM. 2015. Rapid percolation of water through soil macropores affects reading and calibration of large encapsulated TDR sensors. *Soil and Water Research* (in press).

Durner W. 1994. Hydraulic conductivity estimation for soils with heterogeneous pore structure. *Water Resources Research* **32**: 211–223, 1994.

van Genuchten MT. 1980. A closed-form equation for predicting the hydraulic conductivity of unsaturated soils. *Soil Science Society of America Journal* **44**: 892–898.

Gerke H. 2006. Preferential flow descriptions for structured soils. *Journal of Plant Nutrition and Soil Science* **169**: 382–400. DOI:10.1002/jpln.200521955.

Gerke HH, Germann P, Nieber J. 2010. Preferential and unstable flow: from the pore to the catchment scale. *Vadose Zone Journal* **9**: 207–212. DOI:10.2136/vzj2010.0059.

Ireson AM, Wheater HS, Butler AP, Mathias SA, Finch J, Cooper JD. 2006. Hydrological processes in the chalk unsaturated zone – insights from an intensive field monitoring programme. *Journal of Hydrology* **330**: 29–43. DOI:10.1016/j.jhydrol.2006.04.021.

IUSS Working Group WRB. 2006. World reference base for soil resources 2006. A framework for international classification, correlation and communication. *World Soil Resources Reports* **103**. FAO: Rome; 128. ftp://ftp.fao.org/agl/agll/docs/wsrr103e.pdf, September 19, 2013.

J & S Instruments, Inc. 2010. Remotely measure soil moisture with AQUA-TEL-TDR sensor. http://www.jsinstruments.com/files/TDR.pdf, October 18,2014).

Jarvis NJ. 2007. A review of non-equilibrium water flow and solute transport in soil macropores: principles, controlling factors and consequences for water quality. *European Journal of Soil Science* **58**: 523–546. DOI:10.1111/j.1365-2389.2007.00915.x.

Jarvis NJ, Larsbo M. 2012. MACRO (V5.2): model use, calibration and validation. *Transactions of the American Society of Agricultural and Biological Engineers* **55**: 1413–1423. DOI: 10.13031/2013.42251.

Knight JH, Ferré PA, Rudolph DL, Kachanoski RG. 1997. A numerical analysis of the effects of coatings and gaps upon relative dielectric permittivity measurement with time domain reflectometry. *Water Resources Research* **33**: 1455–1460. DOI:10.1029/97WR00435.

Köhne JM, Köhne S, Mohanty BP, Šimůnek J. 2004. Inverse mobile-immobile modeling of transport during transient flow: effects of between-domain transfer and initial water content. *Vadose Zone Journal* **3**: 1309–1321.

Köhne JM, Köhne S, Šimůnek J. 2009. A review of model applications for structured soils: a) water flow and tracer transport. *Journal of Contaminant Hydrology* **104**: 4–35. DOI:10.1016/j.jconhyd.2008.10.002.

Mathias SA, Butler AP, Jackson BM, Wheater HS. 2006. Transient simulations of flow and transport in the chalk unsaturated zone. *Journal of Hydrology* **330**: 10–28. DOI:10.1016/j.jhydrol.2006.04.010.

Moysey SMJ, Liu Z. 2012. Can the onset of macropore flow be detected using electrical resistivity measurements? *Soil Science Society of America Journal* **76**: 10–17. DOI:10.2136/sssaj2010.0413.

Nedvěd V, Balík J, Černý J, Kulhánek M, Balíková M. 2008. The changes of soil nitrogen and carbon contents in a long-term field experiment under different systems of nitrogen fertilization. *Plant, Soil and Environment* **54**: 463–470.

Nolz R. 2013. Performance assessment of selected devices for monitoring soil water balance components with respects to agricultural water management. Dissertation – Institut für Hydraulik und landeskulturelle Wasserwirtschaft (IHLW), BOKU-Universität für Bodenkultur: Wien; 99. https://forschung.boku.ac.at/fis/suchen.hochschulschriften_info?sprache_in=de&menue_id_in=206&id_in=&hochschulschrift_id_in=10871, June 22, 2013.

Oberdörster C, Vanderborght J, Kemna A, Vereecken H. 2010. Investigating preferential flow processes in a forest soil using time domain reflectometry and electrical resistivity tomography. *Vadose Zone Journal* **9**: 350–361. DOI:10.2136/vzj2009.0073.

Pirastru M, Niedda M. 2010. Field monitoring and dual permeability modelling of water flow through unsaturated calcareous rocks. *Journal of Hydrology* **392**: 40–53. DOI:10.1016/j.jhydrol.2010.07.045.

Rosenbaum U, Bogena HR, Herbst M, Huisman JA, Peterson TJ, Weuthen A, Western AW, Vereecken H. 2012. Seasonal and event dynamics of spatial soil moisture patterns at the small catchment scale. *Water Resources Research* **48**: W10544. DOI: 10.1029/2011WR011518.

Sentek. 2003. Access tube installation guide for EnviroSCAN, EnviroSMART, Diviner 2000. Version 1.0. Sentek Pty Ltd.: Stepney, South Australia; 54. http://s.campbellsci.com/documents/us/manuals/sentek_guidev1.pdf, October 27, 2013.

Šimůnek J, van Genuchten MT. 2008. Modeling nonequilibrium flow and transport processes using HYDRUS. *Vadose Zone Journal* **7**: 782–797. DOI:10.2136/vzj2007.0074.

Šimůnek J, Jarvis NJ, van Genuchten MT, Gärdenäs A. 2003. Review and comparison of models for describing non-equilibrium and preferential flow and transport in the vadose zone. *Journal of Hydrology* **272**: 14–35. PII: S0022-1 694(02)00252-4.

Šimůnek J, Genuchten MT, Šejna M. 2012. HYDRUS – the HYDRUS software package for simulating the two- and three-dimensional movement of water, heat, and multiple solutes in variably-saturated media (technical manual, version 2.0). PC-progress: Prague; 258.

Soil Survey Staff. 1999. Soil Taxonomy. A Basic System of Soil Classification for Making and Interpreting Soil Surveys. (2nd edn). *Agriculture Handbook* **436**. United States Department of Agriculture, Natural Resources Conservation Service: Washington, DC; 870. http://www.nrcs.usda.gov/wps/portal/nrcs/detail/soils/survey/publication/?cid=nrcs142p2_053577, February 23, 2015.

Umarova AB, Samoilov OA. 2011. The study of preferential water flows and convective heat transfer using the method of temperature labeling. *Eurasian Soil Science* **44**: 670–676. DOI:10.1134/S1064229311060160.

Wagner A. 2009. Literature study on the correction of precipitation measurements. FutMon C1-Met-29(BY). LWF - Bayerische Landesanstalt für Land und Forstwirtschaft: Freising; 32. http://www.futmon.org/sites/default/files/documenten/Correction_of_precipitation_measurements.pdf, October, 27, 2013.

Zhao X, Voice T, Hashsham SA. 2006. Bioreactor landfill research and demonstration project Northern Oaks Landfill, Harrison, MI. Final Report. Michigan State University **63**. http://www.automata-inc.com/Assets/pdf/Reports/ Bioreactor_Landfill_Final_Report-Harrison-Michigan.pdf, June 2, 2012.

